



Chojnicki, K. N., Clarke, A. B., Phillips, J. C., & Adrian, R. J. (2015). The evolution of volcanic plume morphology in short-lived eruptions. *Geology*, 43(8), 707-710. DOI: 10.1130/G36642.1

Peer reviewed version

License (if available):  
Other

Link to published version (if available):  
[10.1130/G36642.1](https://doi.org/10.1130/G36642.1)

[Link to publication record in Explore Bristol Research](#)  
PDF-document

This is the author accepted manuscript (AAM). The final published version (version of record) is available online via Geological Society of America at <http://geology.gsapubs.org/content/43/8/707>. Please refer to any applicable terms of use of the publisher.

## University of Bristol - Explore Bristol Research

### General rights

This document is made available in accordance with publisher policies. Please cite only the published version using the reference above. Full terms of use are available:  
<http://www.bristol.ac.uk/pure/about/ebr-terms.html>

# Geology

## The evolution of volcanic plume morphology from short-lived eruptions

--Manuscript Draft--

<b>Manuscript Number:</b>	
<b>Full Title:</b>	The evolution of volcanic plume morphology from short-lived eruptions
<b>Short Title:</b>	The evolution of volcanic plume morphology from short-lived eruptions
<b>Article Type:</b>	Article
<b>Keywords:</b>	explosive eruptions; volcanic plume dynamics; unsteady eruption dynamics; impulsive plumes
<b>Corresponding Author:</b>	Kirsten Chojnicki, Ph.D. Scripps Institution of Oceanography La Jolla, CA UNITED STATES
<b>Corresponding Author Secondary Information:</b>	
<b>Corresponding Author's Institution:</b>	Scripps Institution of Oceanography
<b>Corresponding Author's Secondary Institution:</b>	
<b>First Author:</b>	Kirsten Chojnicki, Ph.D.
<b>First Author Secondary Information:</b>	
<b>Order of Authors:</b>	Kirsten Chojnicki, Ph.D. Amanda B. Clarke Jeremy C. Phillips Ronald J. Adrian
<b>Order of Authors Secondary Information:</b>	
<b>Manuscript Region of Origin:</b>	UNITED STATES
<b>Abstract:</b>	<p>The details of volcanic plume source conditions or internal structure cannot readily be revealed by simple visual images or other existing remote imaging techniques. For example, one predominant observable quantity, the spreading rate, in steady or quasi-steady volcanic plumes is independent of source buoyancy flux. However, observable morphological features of short-duration unsteady plumes appear to be strongly controlled by volcanic source conditions, as inferred from recent work in Chojnicki et al. [2014b]. Here we present a new technique for using simple morphological evolution to extract the temporal evolution of source conditions of short-lived unsteady eruptions. In particular, using examples from Stromboli and Santiaguito volcanoes, we illustrate simple morphologic indicators of a) increasing source injection during the early phase of an eruption; b) onset of source injection decline; and c) the timing of source injection cessation. Combined, these indicators allow estimation of changes in eruption discharge rate, injection duration, and may assist in estimating total mass erupted for a given event. In addition, we show how morphology may provide clues about the vertical mass distribution in these plumes, which could be important for predicting ash dispersal patterns.</p>
<b>Suggested Reviewers:</b>	Jeffrey Johnson JeffreyBJohnson@boisestate.edu Experience in analyzing volcanic plume images.  Gregory Waite gpwaite@mtu.edu Experience analyzing volcanic plume and geophysical observations of volcanic eruptions.  Jacopo Taddeucci

[jacopo.taddeucci@ingv.it](mailto:jacopo.taddeucci@ingv.it)

Experience imaging volcanic plumes and eruptions and interpreting their dynamics.

1                   **The evolution of volcanic plume morphology from short-lived eruptions**

2                   K. N. Chojnicki<sup>1</sup>, A. B. Clarke<sup>2</sup>, J.C. Phillips<sup>3</sup>, R. J. Adrian<sup>2</sup>

3                   <sup>1</sup>Scripps Institute of Oceanography, <sup>2</sup>Arizona State University, <sup>3</sup>University of Bristol

4   **Abstract**

5   The details of volcanic plume source conditions or internal structure cannot readily be revealed  
6   by simple visual images or other existing remote imaging techniques. For example, one  
7   predominant observable quantity, the spreading rate, in steady or quasi-steady volcanic plumes is  
8   independent of source buoyancy flux. However, observable morphological features of short-  
9   duration unsteady plumes appear to be strongly controlled by volcanic source conditions, as  
10   inferred from recent work in Chojnicki et al. [2015]. Here we present a new technique for using  
11   simple morphological evolution to extract the temporal evolution of source conditions of short-  
12   lived unsteady eruptions. In particular, using examples from Stromboli and Santiaguito  
13   volcanoes, we illustrate simple morphologic indicators of a) increasing source injection during  
14   the early phase of an eruption; b) onset of source injection decline; and c) the timing of source  
15   injection cessation. Combined, these indicators allow estimation of changes in eruption  
16   discharge rate, injection duration, and may assist in estimating total mass erupted for a given  
17   event. In addition, we show how morphology may provide clues about the vertical mass  
18   distribution in these plumes, which could be important for predicting ash dispersal patterns.

## 19 **1. Introduction**

20 Three classes of volcanic plumes can be differentiated by the relationship between two  
21 time scales, the eruption duration and rise time [e.g., *Sparks et al.*, 1997]. The eruption duration  
22 is the time over which material is injected into the plume. The rise time is the time over which  
23 the plume reaches its maximum height. Plumes with short rise times relative to long eruption  
24 (injection) durations are classified as sustained or steady columns. Plumes with long rise times  
25 relative to the nearly instantaneous duration of explosions are classified as thermals. The third  
26 class of plumes is intermediate to the first two and is characterized by plume rise times that are  
27 comparable to short eruption durations. Plumes in this class are short-lived and highly unsteady.  
28 Each class exhibits a distinct relationship between the eruption (or injection) conditions and the  
29 plume rise dynamics that control plume morphology.

30 Sustained volcanic columns tend to have conical geometries [e.g., *Wilson*, 1976; *Sparks*  
31 *et al.*, 1997], and volcanic thermals tend to have approximately spherical geometries [e.g.,  
32 *Wilson*, 1976; *Sparks et al.*, 1997]. Both of these geometries are thought to indicate that the  
33 plume is in a self-similar dynamic state (i.e., the flow morphology does not change in time), and  
34 that the flow can be described reasonably well with analytical models that approximate the  
35 detailed turbulent dynamics [*Morton et al.*, 1956]. According to these models, the rise of  
36 sustained volcanic columns is primarily controlled by the rate at which buoyant fluid is  
37 discharged into the plume; on the other hand, thermals are controlled by the total amount of  
38 buoyant discharged fluid, not the discharge rate [e.g., *Morton et al.*, 1956; *Wilson*, 1976; *Sparks*  
39 *et al.*, 1997].

40 Intermediate volcanic plumes take on a variety of morphologies [e.g., *Patrick*, 2007].  
41 These include features that are spherical and conical, as well as cylindrical [*Patrick*, 2007].

42 These morphologic characteristics also evolve over time, changing throughout the plume rise  
43 process [e.g., *Patrick, 2007; Mori and Burton, 2009; Chojnicki et al., 2015*]. The morphologies  
44 are not well understood and lack analytical descriptions, but here we seek a method of inferring  
45 the dynamic flow conditions in these intermediate plumes and the factors that control them using  
46 observations of their morphological evolution.

47 The initial rise of volcanic plumes before they reach their maximum height and form a  
48 conical column has been modeled as a ‘starting plume’ [*Turner, 1962 Wilson and Self, 1980;*  
49 *Sparks and Wilson, 1982; Patrick, 2007*]. According to this description, the starting plume has  
50 two prominent features, a spherical head and a conical tail. The dynamics are different in each  
51 feature. The spherical head contains a starting vortex structure and the conical tail contains a  
52 steady jet structure [*Turner, 1969*]. While this model appears to capture some aspects of  
53 intermediate volcanic plume morphology, such as the presence of spherical heads [*Chojnicki et*  
54 *al., 2015*], it cannot explain the cylindrical geometry of some plumes such as those identified by  
55 Patrick [2007].

56 Kitamura and Sumita [2011] attribute these cylindrical features to unsteadiness in  
57 discharge conditions after finding they could not reproduce the cylindrical features in analogue  
58 laboratory jets evolving from a steady rate of buoyant discharge. Our previous laboratory  
59 experiments support this claim, as we were able to generate neutrally buoyant analogue jets with  
60 cylindrical geometries using an unsteady discharge rate [*Chojnicki et al., 2015*]. We observed the  
61 evolution of both the analogue jet morphology and the internal velocity fields and found that the  
62 analogue jet morphology is a good indicator of the jet internal velocity structure and dynamics.  
63 Furthermore, and most importantly, we found that changes in the analogue jet morphology  
64 correlate well with changes in the discharge rate. We therefore apply our laboratory analysis to

65 observations of volcanic plumes to show how morphology may be used as an indicator of  
66 discharge conditions for intermediate plumes. Because ground-based observations of volcanic  
67 plumes from short eruptions (tens to hundreds of seconds) are becoming increasingly common  
68 [*Patrick, 2007; Mori and Burton, 2009; Lopez et al., 2013; Valade et al., 2014; Webb et al.,*  
69 *2014*], we anticipate that this approach will be applicable in a wide range of field settings in the  
70 future.

## 71 **2. Analogue Jet Experiments**

72 The analogue jet experiments used here are discussed in detail by Chojnicki et al. [2014,  
73 2015]. We provide a brief summary here. Our experiments were performed under idealized  
74 conditions in the laboratory so that both the jet and the source could be measured simultaneously.  
75 Turbulent jets were generated in the laboratory by injecting water at high-speeds into a tank of  
76 still water through a circular vent. The injection durations were comparable to, but shorter than,  
77 plume rise times, consistent with conditions for intermediate eruption plumes [*Clarke et al.,*  
78 *2009*]. The experimental injection rates varied in a Gaussian-like temporal evolution, consistent  
79 with conditions for short-lived eruptions [*Clarke et al., 2002*], with a total duration of 0.40  
80 seconds. We measured the resultant jet morphology as well as the structure of the internal flow  
81 field using Particle Image Velocimetry [*Chojnicki et al., 2015; following Adrian, 1984*]. The  
82 analogue jets were seeded with silver-coated particles and illuminated by a laser light sheet,  
83 producing the unprocessed PIV images presented in Chojnicki et al. [2015]. The tank water  
84 appears black relative to the seeded jet water, creating a visualization similar to a dyed jet [Panel  
85 a in Figures 1, 2, and 3]. We deem these images to be the best way to simultaneously visualize  
86 jet morphology and the fluid velocity field.

87           The analogue jets created by the Gaussian-form injection rates evolved in three phases  
88 [Chojnicki *et al.*, 2015]. The vent condition during Phase 1 is characterized by an increase in the  
89 injection rate over time. During Phase 1 the jet forms two main regions - a spherical head and a  
90 roughly cylindrical tail (Figure 1a). The spherical head consists of a starting vortex structure  
91 (labeled V1), common in jets moving into still ambient fluids [e.g., Kieffer and Sturtevant,  
92 1984]. The cross-sectional width of the head is larger than the cross-sectional width of the tail.  
93 The tail has two sections, labeled 2 and 3, with cross-sectional widths similar to the starting  
94 vortex (section 2) and the vent (section 3).

95           The vent condition of Phase 2 is characterized by a decrease in the injection rate over  
96 time. The arrival of Phase 2 is indicated by the appearance of a narrow ‘neck’ region between the  
97 starting vortex and section 2 of the cylindrical tail (Figure 2a), which develops as the starting  
98 vortex pulls away from the more slowly injected tail. The propagation of Section 2 slows as it  
99 moves away from source while section 3 continues at the same velocity due to inertia; the two  
100 sections thus start to combine into a conical form in Phase 2.

101           After injection ends, the analogue jet enters Phase 3 (Figure 3a). The arrival of this phase  
102 is indicated by another change in shape of the jet. Section 2 has formed a vortex and become the  
103 wide head of the jet, while Sections 3 and 4 form the jet tail, which is now cylindrical-to-conical  
104 in shape. The tail is disconnected from the vent as evidenced by the presence of ambient fluid  
105 between the vent and jet tail. The internal velocity structure of the jet re-organizes during this  
106 phase from the elongated pattern characterizing the cylindrical geometry to the compact radial  
107 pattern characterizing a spherical geometry [not shown; Chojnicki *et al.*, 2015]. The original  
108 starting vortex V1 has moved completely independently of the tail, leaving the field of view.

### 109 **3. Volcanic Plume Analysis**



110           Although we cannot readily compare the internal velocity field results from Chojnicki et  
111 al., [2015] with observations of opaque volcanic plumes, we can compare the morphologies of  
112 our analogue jets to volcanic plumes. One study in the literature was suitable for this type of  
113 analysis because it provided information about the evolution of plume behavior and estimates for  
114 ash and gas contents. This study was from a hornito event at Stromboli and observed with an  
115 ultraviolet camera [*Mori and Burton, 2009*]. The plume observations (Panel b in Figures 1, 2 and  
116 3) are modified from Mori and Burton [2009] and use a false-color scale where light grey  
117 represents high concentrations of sulfur dioxide and/or volcanic ash, dark grey represents lower  
118 concentrations, indicative of mixing of the plume fluid and ambient air, and black represents the  
119 zero concentration of pure ambient air.

120           Mori and Burton [2009] classify this event as Type 2 [*Patrick, 2007*], an ashy plume with  
121 a rise behavior that decelerates from an initially high velocity and then rises at a constant rate.  
122 These events are interpreted to have momentum as the primary driver during the initial stages  
123 when the flow-front propagation is decelerating [*Patrick, 2007*]. Thus, we assume buoyancy is  
124 not a dominant driver of the volcanic plume near the vent. Mori and Burton [2009] note that an  
125 ambient wind was present during this event, but given that the plume axis is near-vertical we  
126 argue that wind has at most a secondary effect in the initial rise process. We therefore assume  
127 our experimental results, with a neutrally buoyant jet rising into a still ambient, are analogous, at  
128 least to a first approximation.

129           For the first 8s of the Stromboli eruption (Figure 1b), a round head and a cylindrical tail  
130 characterize the plume morphology. The cylindrical tail can be subdivided into two sections: one  
131 with a width similar to the head (section 2) and one that has a smaller width (section 3). This  
132 simplified morphology is easy to distinguish in the volcanic plume images despite their greater

133 complexity relative to the simple analogue jets. This morphology corresponds with Phase 1 in  
134 analogue jet evolution (Figure 1a), during which the vent discharge is increasing (source  
135 acceleration stage) [Chojnicki *et al.*, 2015]. Thus, we also infer that the vent discharge rate is  
136 increasing during the first 8 s of this Stromboli. This inference is consistent with the  
137 interpretations of increasing gas flux made by Mori and Burton [2009]. We also observe in the  
138 laboratory experiments during Phase 1 that section 3 of the cylindrical tail has a similar diameter  
139 as the vent. We thus infer that the diameter of the volcanic plume tail (section 3) of ~6 meters is  
140 similar to the diameter of the volcanic vent. This inference is reasonably consistent with  
141 independent evidence that the hornito vents are approximately 2-5 meters wide [Chouet *et al.*,  
142 1974; Vergnolle and Brandeis, 1996; Del Bello *et al.*, 2012].

143         We cannot state without uncertainty that the cylindrical shape of the jets during Phase 1  
144 is uniquely indicative of an increasing discharge rate. However, we do assert that the cylindrical  
145 shape may be a good indicator of source unsteadiness, given that the cylindrical geometry  
146 appears in our analogue jets when the ejection is Gaussian in time, but cylindrical geometry is  
147 not observed when the source is steady as in Kitamura and Sumita [2011]. Given this ambiguity,  
148 future work should examine jet morphology response to a wide range of temporally varying  
149 discharge histories to determine if the cylindrical shape is unique to the discharge condition  
150 inferred here.

151         Snap shots of the Stromboli plume at 10s and 12s are shown in Figure 2b (right two  
152 panels). At these times a narrow neck of fluid begins to form between the head and tail of the  
153 volcanic plume. We infer this narrow region to be similar to the neck in the analogue jets that  
154 appears in Phase 2 (Figure 2a). This neck first appears when the discharge rate begins to  
155 decrease in the laboratory experiments [start of the falling edge of the Gaussian injection;

156 *Chojnicki et al.*, 2015]. We therefore infer that the discharge rate has begun to decrease by this  
157 point in the volcanic eruption as well. This inference is not consistent with the interpretations of  
158 the gas flux made by Mori and Burton [2009], in which they conclude that discharge rate should  
159 still be increasing at this time. However, they assume that the total amount of sulfur dioxide in  
160 the image is a good proxy for the discharge conditions. We argue instead that the total amount of  
161 discharged sulfur dioxide (the amount in the images) is a proxy for the cumulative mass of fluid  
162 discharged from the beginning of the eruption until the time of the measurement, rather than a  
163 good indicator of the instantaneous discharge rate.

164         Snapshots of the plume from 14s to 20s are shown in Figure 3b. Although the shape of  
165 the plume near the volcanic vent is difficult to see, we note a rounded feature near the base of the  
166 plume, designated as the End Vortex (labeled EV) below which the plume narrows and nearly  
167 pinches out. The development of the EV is also observed in ‘stopping jets’ that are buoyant  
168 [*Kattimeri and Scase*, 2014]. In the analogue jet during Phase 3 (Figure 3a), there is also a gap  
169 between the base of the tail and the vent, while the EV is more difficult to observe. This gap  
170 appears between the vent and the EV in the volcanic plume (Figure 3b) and, thus, we interpret  
171 the EV to mark the end of the injection. The EV first appears at 12s (Figure 2b) in the volcanic  
172 eruption suggesting that the discharge rate decreased and ended around this time.

173         These combined observations indicate that the volcanic plume entered Phase 3 by  
174 approximately 14s after onset. In this phase of the analogue jets (Figure 3a), the starting vortex  
175 evolves independently of the tail. Evidence for this same independent motion in the volcanic  
176 plume is found in the difference in the concentrations between section 2 and V1 (Figure 3b); the  
177 concentration decreases over time in V1 but remains similar over time in section 2 and V1  
178 appears to be moving or ‘stretching’ away from section 2. Furthermore, the concentration

179 appears to decrease over time in sections 3 and 4 as well, but at a slower rate than the decrease in  
180 V1. These analogous observations of the laboratory jets indicate that the dynamics in different  
181 parts of the flow evolve somewhat independently in the later stages of the plume evolution. The  
182 spatial variations in plume evolution, and corresponding variations in plume dilution, are  
183 important considerations when modeling the dynamics of these plumes and resultant ash  
184 dispersal.

185         Phase 3 of the analogue jet evolution is marked by the particular characteristics of section  
186 2, and the volcanic plume appears to follow a similar evolution (Figure 3). In Figure 3 section 2  
187 appears to contain the highest fluid concentrations in both the laboratory (Figure 3a) and  
188 Stromboli (Figure 3b) flows. This pattern has implications for the transport of mass by the  
189 volcanic plume as it dissipates. In the laboratory case, and possibly also in the Stromboli case,  
190 the lower second structure appears to contain most of the mass within the plume, making the  
191 plume height an unreliable indicator of the height of the largest concentration of ash released to  
192 the atmosphere for subsequent downwind transport. Although, the difference in position between  
193 the second structure and flow front is small in this hornito event, it could be larger, and more  
194 significant, in larger short-duration events or as the plume evolves in time and grows in height.

195         In addition to the hornito event at Stromboli, we document the evolution of a single event  
196 at Santiaguito volcano in Guatemala (Figure 4), which is also known for generating short-  
197 duration explosive events, although the magma composition and thus exact eruption mechanisms  
198 are thought to vary between the two volcanoes. The images in Figure 4 were collected in January  
199 2012 using a PlotWatcher Pro time-lapse camera sampling at 1 frame per second from the  
200 summit of Santia Maria.

201 We observe similar plume evolution at Santiaguito and Stromboli. The round front and  
202 tail regions of variable widths supply evidence for the generation of several features documented  
203 in the analogue jets - the starting vortex as well as the second, third, and fourth dynamic regions  
204 (as labeled in Figure 4). Unlike the Stromboli plume and analogue jets, however, no neck forms  
205 in the Santiaguito plume. The neck may not form for a variety of reasons including the absence  
206 of a discharge decrease in this event or perhaps the strong influence of buoyancy forces in the  
207 plume that cause section 2 to accelerate into V1, preventing the separation of the first structure  
208 from the second. Another characteristic unique to the Santiaguito plume is the appearance of the  
209 fourth dynamic region that is more cylindrical than conical. This region is identified here by the  
210 fact that its visible boundary is less clearly defined as compared with regions V1 through 3,  
211 possibly suggesting different dynamics at work in that region, such as a more gradual ending to  
212 the injection.

#### 213 **4. Conclusions**

214 Under unsteady discharge conditions, analogue jets and short-eruption volcanic plumes  
215 evolve as a sequence of distinct flow segments. The segments grow in height and width, at  
216 various rates, as they rise. For analogue jets, changes in in the flow morphology can be  
217 correlated to changes in discharge conditions. Thus, the possibility exists to use changes in  
218 volcanic plume morphology as an indicator of changes in eruption discharge rate, and estimation  
219 of injection duration (and eventually mass eruption rate or total mass erupted) [*Chojnicki et al.*,  
220 2015]. Inferring source conditions from relatively easy- and safe-to-collect plume observations  
221 may also reduce ambiguity in interpreting geophysical observations of eruption activity, when  
222 geophysical data is available, and provide a means of monitoring the evolution of eruption  
223 source conditions when geophysical data is not available or not available in real-time. Similar

224 patterns of morphology evolution are observed for short-eruption volcanic plumes from  
225 Santiaguito and Stromboli volcanoes. We therefore suggest that plumes from short-lived  
226 eruptions with transient discharges will generally evolve in a similar way. More work on the  
227 effects of buoyancy and different discharge histories is needed to improve these inferences.

## 228 **Acknowledgements**

229         This work was supported by the National Science Foundation under grants EAR 0810258  
230 and EAR 0930703 and by the Fulton Endowment. Contact K. Chojnicki or A. Clarke to request  
231 data. K.C. acknowledges Jeff Johnson and Ben Andrews for assistance in collecting the  
232 Santiaguito plume images.

233

233 **References**

- 234 Adrian, R. J. (1984) Scattering particle characteristics and their effect on pulsed laser  
235 measurements of fluid flow: speckle velocimetry vs. particle image velocimetry, *Applied*  
236 *optics*, 23, 1690 -1691,doi:10.1364/AO.23.001690.
- 237 Chojnicki, K. N., A. B. Clarke, R. J. Adrian, and J. C. Phillips, (2014), The flow structure of jets  
238 from transient sources and implications for modeling short-duration explosive volcanic  
239 eruptions, *Geophysics, Geochemistry, Geosystems*, 15, doi: 10.1002/2014GC005471.
- 240 Chojnicki, K. N., A. B. Clarke, J. C. Phillips, R. J. Adrian (2015), Rise dynamics of unsteady  
241 laboratory jets with implications for volcanic plumes, *Earth and Planetary Science*  
242 *Letters*, 412, 186-196, doi:10.1016/j.epsl.2014.11.046.
- 243 Chouet, B., N. Hamisevich, and T. R. McGetchin (1974), Photoballistics of volcanic jet activity  
244 at Stromboli, Italy, *Journal of Geophysical Research*, 79(32), 4961–4976,  
245 doi:10.1029/JB079i032p04961.
- 246 Clarke, A. B., A. Neri, G. Macedonio, B. Voight, and T. H. Druitt (2002), Computational  
247 modeling of the transient dynamics of the August 1997 Vulcanian explosions at Soufriere  
248 Hills volcano, Montserrat influence of initial conduit conditions on near-vent pyroclastic  
249 dispersal, In: Druitt, T. H. & Kokelaar, B. P. (eds) *The Eruption of the Soufrière Hills*  
250 *Volcano, Montserrat, from 1995 to 1999*. Geological Society, London, *Memoirs* 21, 319–  
251 348.
- 252 Clarke, A. B., J. C. Phillips, and K. N. Chojnicki (2009), An investigation of Vulcanian eruption  
253 dynamics using laboratory analogue experiments and scaling analysis, From: Thordarson,  
254 T., Self, S., Larsen, G., Rowland, S. K. & Hoskuldsson, A. (eds) *Studies in Volcanology:*

255 The Legacy of George Walker. Special Publications of IAVCEI. 2, 155–166. Geological  
256 Society, London.

257 Del Bello, E., E. W. Llewellyn, J. Taddeucci, P. Scarlato, and S. J. Lane (2012), An analytical  
258 model for gas overpressure in slug-driven explosions: Insights into Strombolian volcanic  
259 eruptions, *Journal of Geophysical Research*, 117, B02206, doi:10.1029/2011JB008747.

260 Kattimeri, A., and M. M. Scase (2014), Turbulent ‘stopping plumes’ and plume pinch-off in  
261 uniform surroundings, *Environmental Fluid Mechanics*, doi:10.1007/s10652-014-9387-7.

262 Kieffer, S. and B. Sturtevant (1984), Laboratory Studies of Volcanic Jets, *Journal of Geophysical*  
263 *Research*, 89, B10, 8253-8268, doi: 10.1029/JB089iB10p08253.

264 Kitamura, S., and I. Sumita (2011), Experiments on a turbulent plume: Shape analyses, *Journal*  
265 *of Geophysical Research*, 116, B03208, doi:10.1029/2010JB007633.

266 Lopez, T., D. Fee, F. Prata, and J. Dehn (2013), Characterization and interpretation of volcanic  
267 activity at Karymsky Volcano, Kamchatka, Russia, using observations of infrasound,  
268 volcanic, Geochemistry, Geophysics, Geosystems, emissions, and thermal imagery, 14,  
269 doi:10.1002/2013GC004817.

270 Mori, T., and M. Burton (2009), Quantification of the gas mass emitted during single explosions  
271 on Stromboli with the SO<sub>2</sub> imaging camera, *Journal of Volcanology and Geothermal*  
272 *Research*, 188, 395 – 400. doi:10.1016/j.jvolgeores.2009.10.005.

273 Morton, B. R., G. Taylor, and J. S. Turner (1956), Turbulent gravitational convection from  
274 maintained and instantaneous sources, *Proceedings of the Royal Society of London*  
275 *Series A*, 234, 1-23, doi:10.1098/rspa.1956.0011.



276 Patrick, M. R. (2007), Dynamics of Strombolian ash plumes from thermal video: Motion,  
277 morphology, and air entrainment, *Journal of Geophysical Research*, 112, B06202,  
278 doi:10.1029/2006JB004387.

279 Sparks, R. S. J., M. I. Bursik, S. N. Carey, J. S. Gilbert, L. S. Glaze, H. Sigurdsson, and A. W.  
280 Woods (1997), *Volcanic Plumes*, 524 pp., John Wiley, New York.

281 Sparks, R. S. J., and L. Wilson (1982), Explosive volcanic eruptions–V. Observations of plume  
282 dynamics during the 1979 Soufriere eruption, St. Vincent, *Geophysical Journal*  
283 *International*, 69(2), 551– 570, doi:10.1111/j.1365-246X.1982.tb04965.x.

284 Turner, J. S. (1962), The ‘starting plume’ in neutral surroundings, *Journal of Fluid Mechanics*,  
285 13, 356 – 358, doi:10.1017/S0022112062000762.

286 Turner, J. S. (1969), Buoyant plumes and thermals, *Annual Review of Fluid Mechanics*, 1, 29-  
287 44, doi: 10.1146/annurev.fl.01.010169.000333.

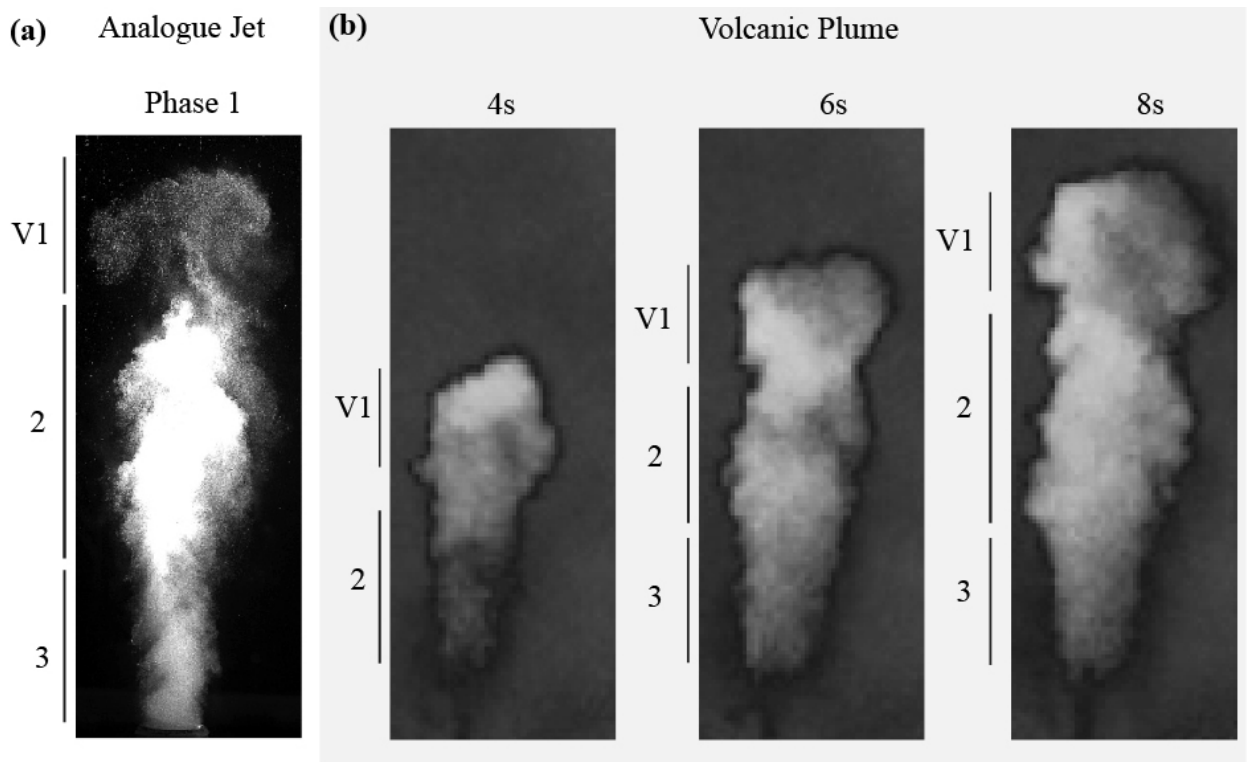
288 Valade, S. A., A.J.L. Harris, M. Cerminara (2014), Plume Ascent Tracker: Interactive Matlab  
289 software for analysis of ascending plumes in image data, *Computers & Geosciences*, 66,  
290 132-144, doi:10.1016/j.cageo.2013.12.015.

291 Vergnolle, S., and G. Brandeis (1996), Strombolian explosions: 1. A large bubble breaking at  
292 the surface of a lava column as a source of sound, *Journal of Geophysical Research*,  
293 101(B9), 20,433–20,447, doi:10.1029/96JB01178.

294 Webb, E. B., N. R. Varley, D. M. Pyle, and T. A. Mather (2014), Thermal imaging and analysis  
295 of short-lived Vulcanian explosions at Volcán de Colima, Mexico, *Journal of*  
296 *Volcanology and Geothermal Research*, 278-279, 132-145,  
297 doi:10.1016/j.jvolgeores.2014.03.013.

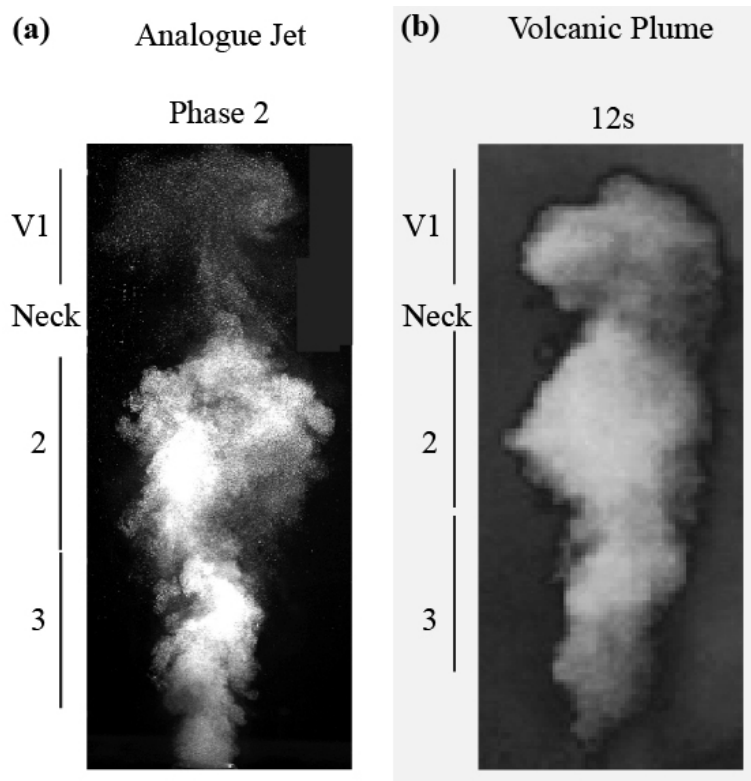
298 Wilson, L. (1976), Explosive volcanic eruptions – III. Plinian eruption columns, *Geophysical*  
299 *Journal International*, 45 (3), 543-556, doi:10.1111/j.1365-246X.1976.tb06909.x  
300 Wilson, L., and S. Self (1980), Volcanic explosion clouds: Density, temperature and particle  
301 content estimates from cloud motion, *Journal of Geophysical Research*, 85, 2567– 2572,  
302 doi: 10.1029/JB085iB05p02567.

303 Figure 1: (a) Analogue jet (white pixels) image characterizing Phase 1 of the jet  
 304 evolution, modified from Chojnicki et al. [2015]. (b) False-color images of an evolving  
 305 volcanic plume from a hornito event at Stromboli, modified from Mori and Burton  
 306 [2009]. Light grey, dark grey and black indicate high, low and zero concentrations of  
 307 sulfur dioxide/volcanic ash, respectively. Labels represent different dynamic regions of  
 308 the flows: V1 is the starting vortex, sections 2 and 3 form the cylindrical tail with a cross  
 309 sectional width similar to the head (2) and vent (3).



310

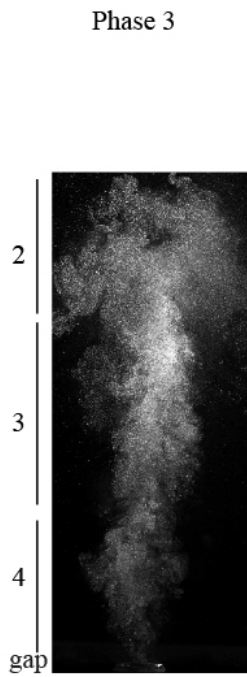
311 Figure 2: (a) The appearance of a ‘neck’ between sections V1 and 2 in analogue jets indicates the  
312 flow has entered phase 2 during which the discharge rate is decreasing [Chojnicki *et al.*, 2015].  
313 (b) The neck is also present in the volcanic plume at 12s [Mori and Burton, 2009] and, thus, we  
314 infer the discharge rate to be decreasing at that time.



315

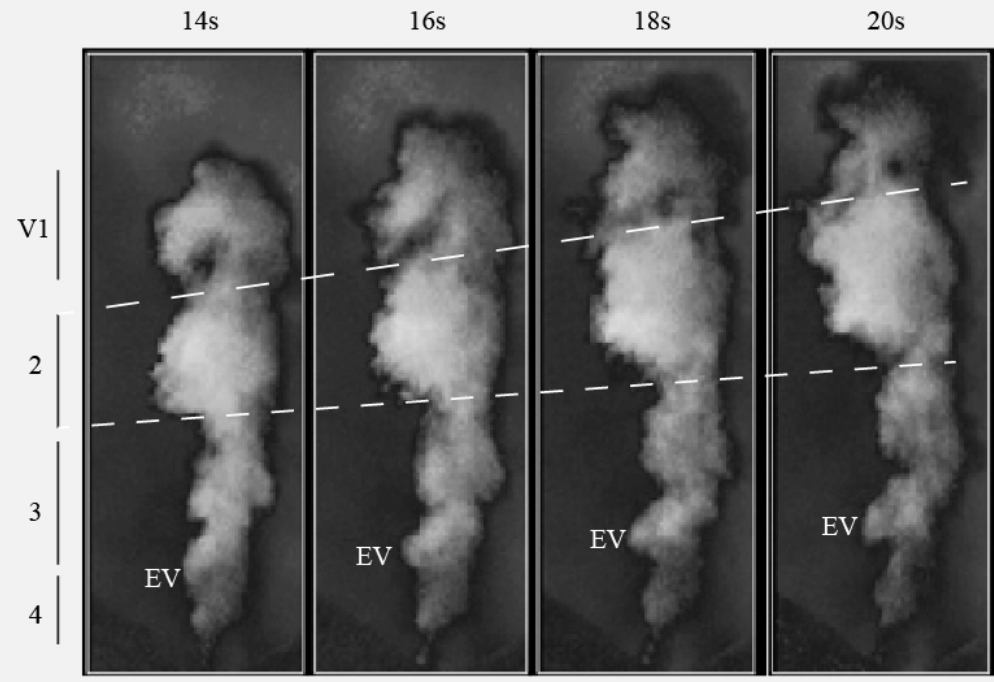
316 Figure 3. (a) In the analogue jets, the appearance of a narrow base, section 4, and a gap between  
 317 the plume and the source indicates the discharge has ended and the flow is in Phase 3 [*Chojnicki*  
 318 *et al.*, 2015]. (b) In the Stromboli plume [*Mori and Burton*, 2009], this is difficult to see but an  
 319 ending vortex (EV) may indicate then end of injection.

**(a) Analogue Jet**



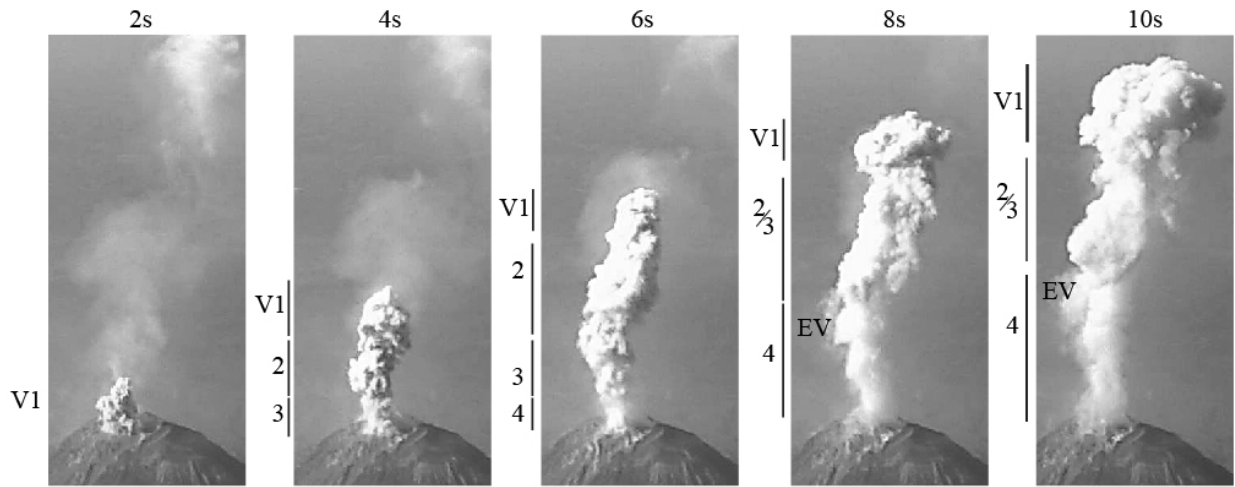
**(b)**

**Volcanic Plume**



320

321 Figure 4. Snap shots of an evolving volcanic plume from Santiaguito volcano in Guatemala  
322 showing similar features to the analogue jets and the Stromboli plume, despite the differences in  
323 the volcanic systems.



324